The following supplement accompanies the article

Maternal size and body condition determine calf growth rates in southern right whales

Fredrik Christiansen*, Fabien Vivier, Claire Charlton, Rhianne Ward, Stephen Burnell, Alicia Amerson, Lars Bejder

*Corresponding author: f.christiansen@murdoch.edu.au

Marine Ecology Progress Series 592: 267–281 (2018)

Supplement 1.

Table S1. Definition of grades (scores) used for each photograph attribute to select body condition photographs for analyses. See Fig. S2 for example pictures of each grade for each attribute.

Attribute	Score 1 (good)	Score 2 (medium)	Score 3 (poor)
(A) Camera focus	The picture is sharp with the contour of the whale's body clearly visible.	The picture is blurry, but still clear enough to make out the contour of the whales body.	The picture is too blurry to make out the contour of the whales body.
(B) Body straightness	The body axis midline crosses the peduncle closer to the centre than to the edges.	The body axis midline crosses the peduncle closer to the edges than to the centre, but does not cross outside the peduncle.	The body axis midline crosses outside the peduncle of the animal.
(C) Body roll	The blowhole of the whale is aligned with the midline body axis of the whale.	The blowhole of the whale deviates slightly (<1/3 of the eye width) from the midline body axis of the animal.	The blowhole of the whale deviates significantly (>1/3 of the eye width) from the midline body axis.
(D) Body arch	No visible arching of the body. The animal is lying vertically flat in the water.	The head or the peduncle/tail region of the animal is slightly lifted or dropped.	The head or the peduncle/tail region of the animal is significantly lifted or dropped, or both the head and the peduncle/tail region is slightly lifted or dropped.
(E) Body pitch	The body axis of the whale is not angled vertically.	The body axis of the whale is angled slightly in the vertical plane, either up or down.	The body axis of the whale is angled significantly in the vertical plane, either up or down.
(F) Body length measurability	Both the tip of the rostrum and the notch of the tail fluke are clearly visible.	The tip of the rostrum or the notch of the tail fluke is unclear or partly obscured, but can still be approximated.	The tip of the rostrum and/or the notch of the tail fluke are not visible due to spray, water distortion, another animal or object, or is too far down in the water column.
(G) Body width measurability	The body contour of the whale is clearly visible.	The body contour of the whale is mostly visible, but some parts of the body are unclear or obscured. Missing parts of the contour can be reliably extrapolated from visible parts of the body.	The body contour of the whale is unclear and obscured to such a degree that extrapolation of the body contour based on visible parts of the body is not possible.

Fig. S1. The Inspire 1 Pro unmanned aerial vehicle and the configuration of the range finder system used in this study. The range finder system was built, fitted and tested by Global Unmanned Systems (www.gus-uav.com).

Fig. S2. Example photos for each photo score (grade) for the different photo attributes used when filtering photographs for body condition analyses: (A) camera focus, (B) body straightness, (C) body roll, (D) body arch, (E) body pitch, (F) body length measurability, (G) body width measurability. See Table S1 for definition of the different grades for each attribute.

(A) Camera focus:

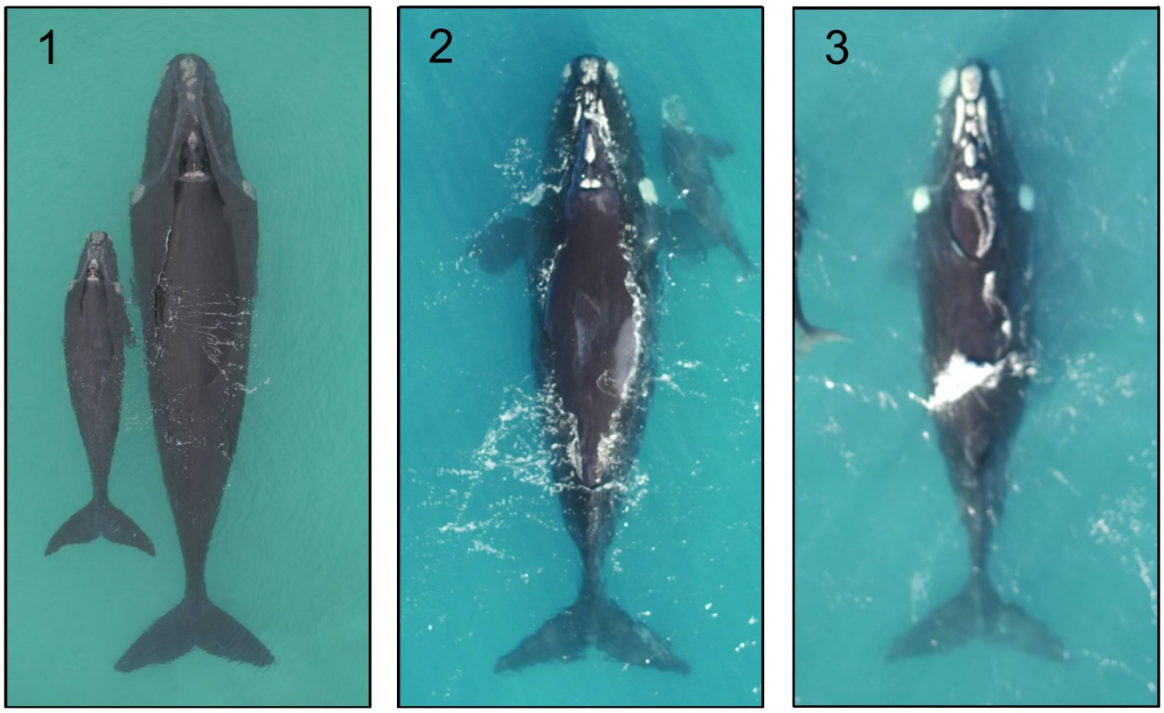

(B) Body straightness:

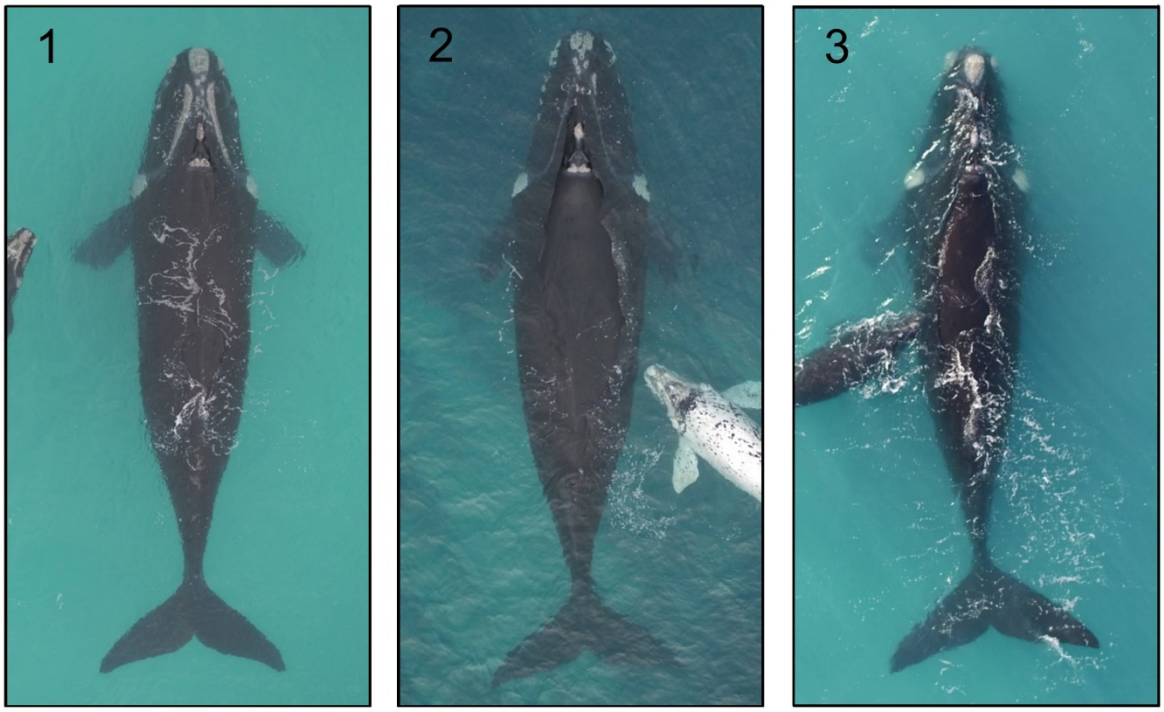

(C) Body roll:

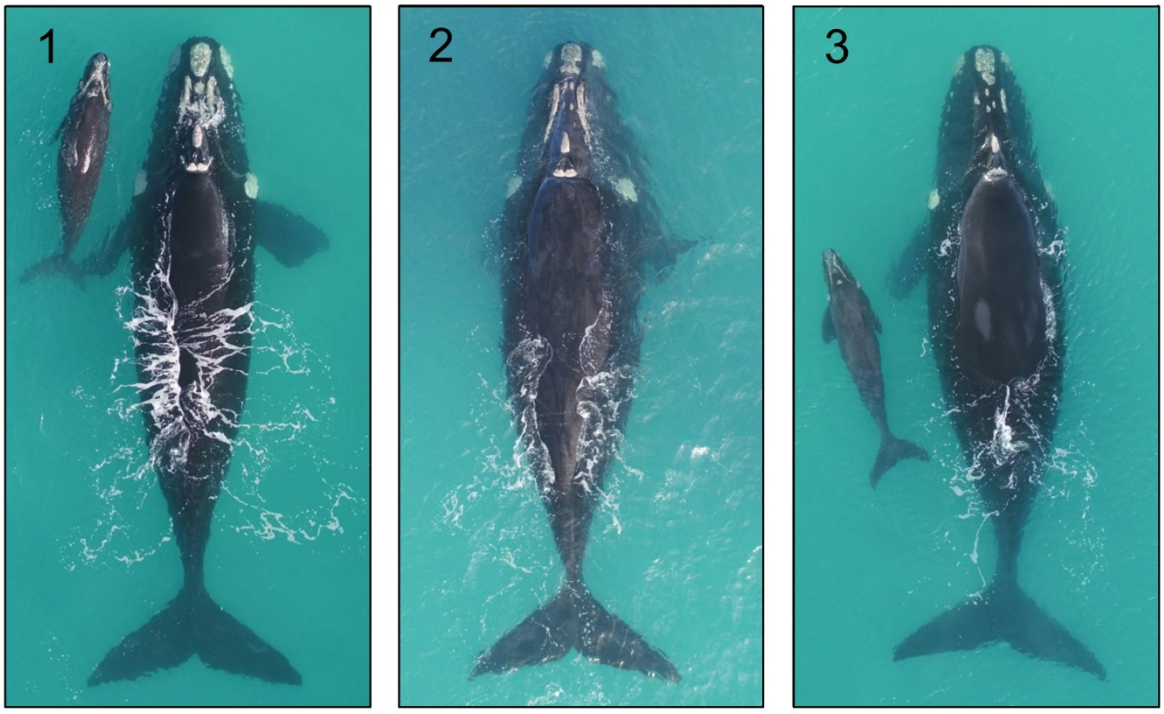

(D) Body arch:

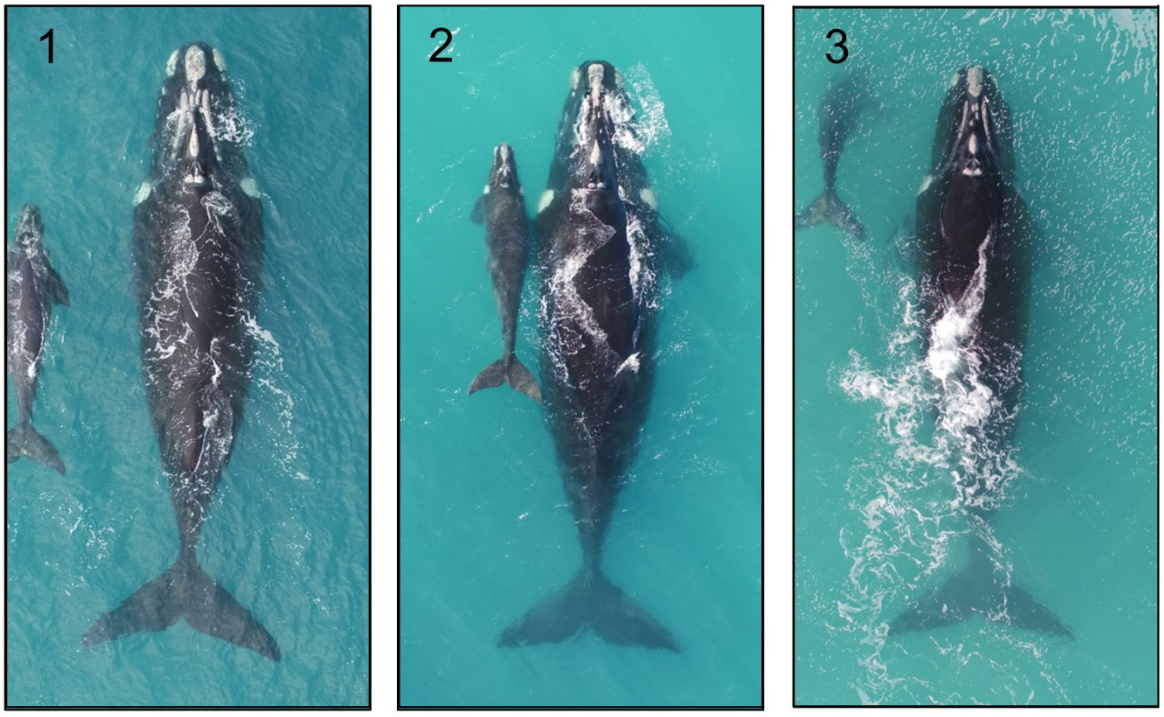

(E) Body pitch:

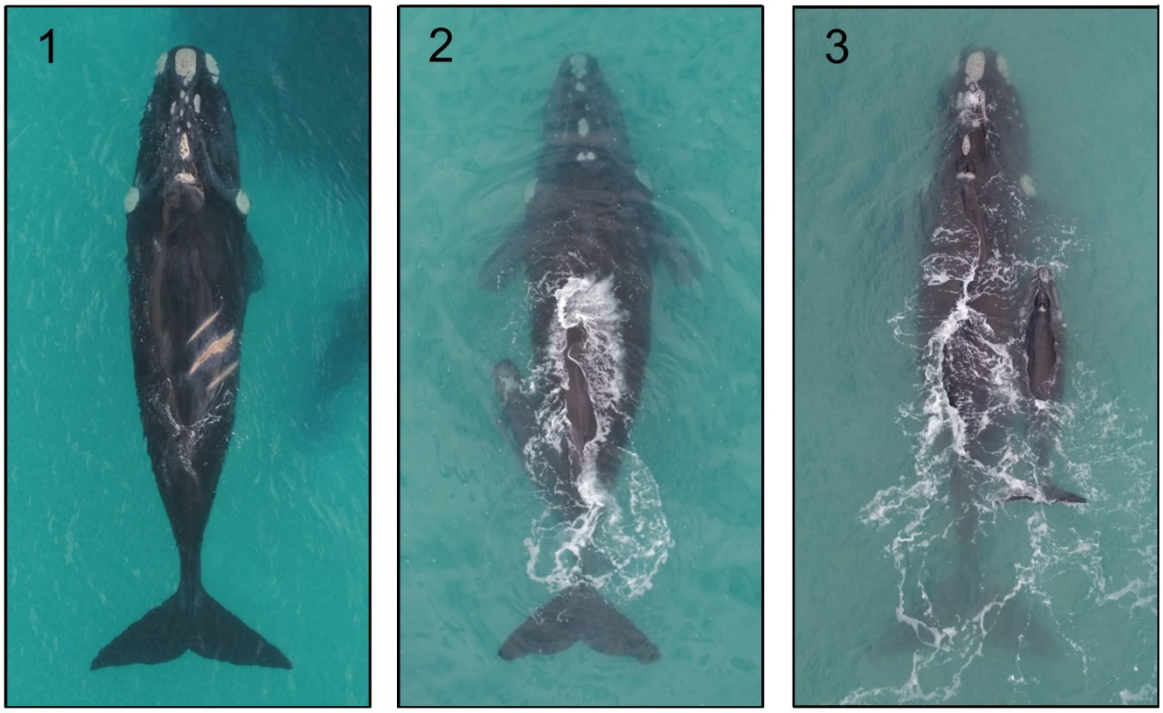

(F) Body length measurability:

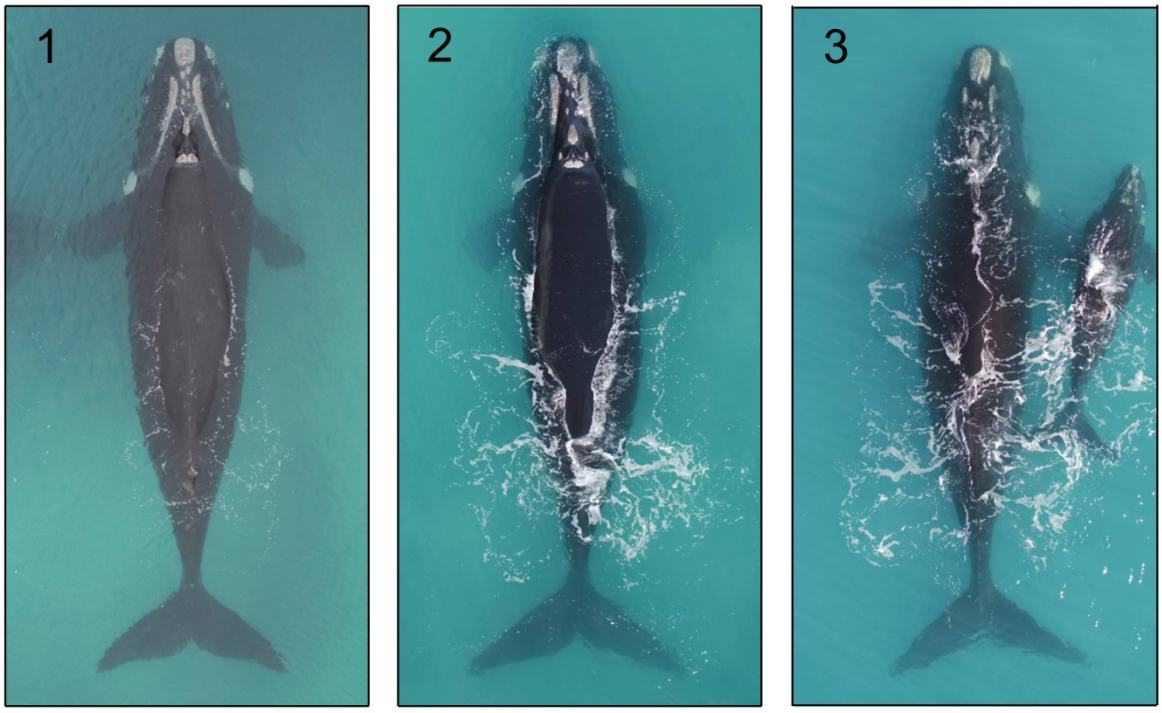

(G) Body width measurability:

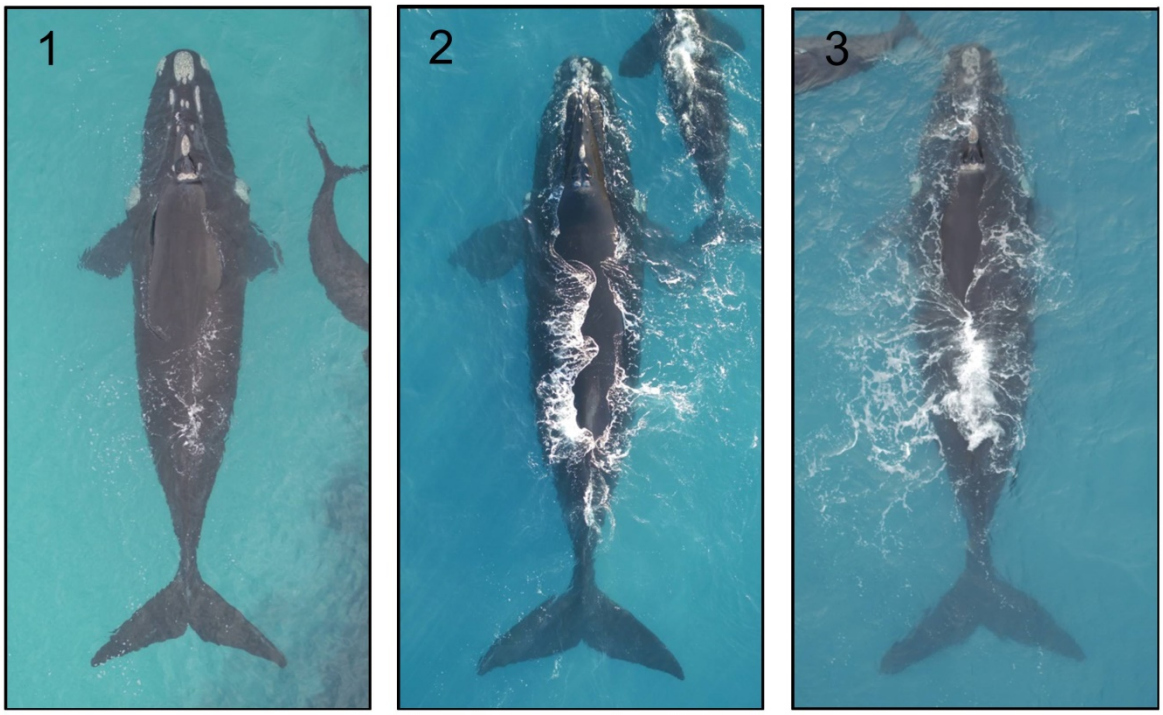

Fig. S3. The relative (proportional) difference between the observed rates of body width change and the median rate of change for each body width measurement site (5-90% from the tip of the rostrum) as a function of (A) duration of the sampling period (number of days between the first and last measurement of an individual) and (B) sample size (total number of measurements of an individual). Eighteen values (one for each measurement site) are provided for each individual female (black points) and calves (red points). A lower threshold of 20 days and 4 data points (red vertical dashed lines) was used to remove individuals from analyses. n=78 individuals.

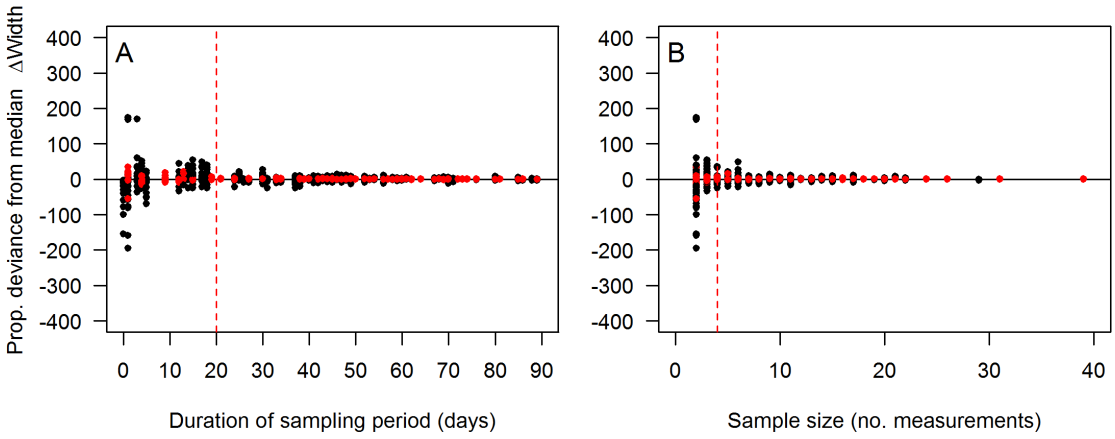

Fig. S4. Boxplots of (A) the proportional size of the head and (B) the relative distance to the start of the tail fluke (measured relative to body length, BL) of southern right whale calves and lactating females. n=1,600 measurements (including repeated measurements from the same individuals).

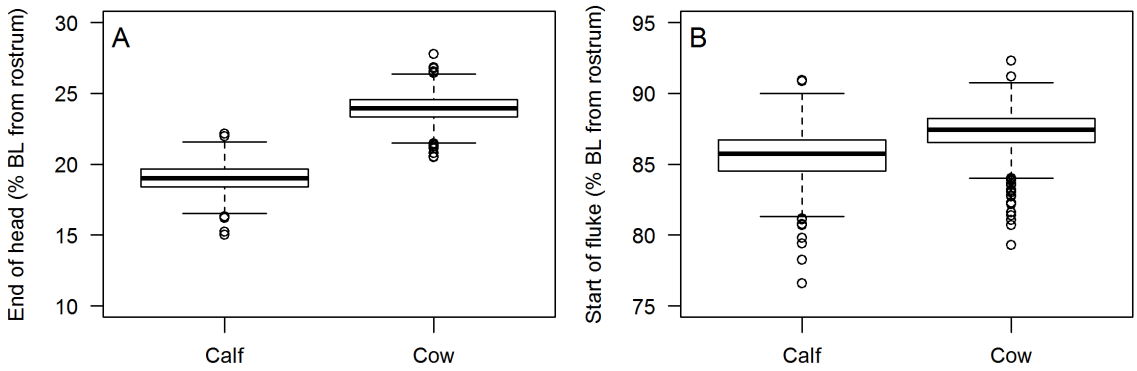

Fig. S5. Frequency distribution of the coefficient of determination (R^2) in rate of change in body volume of individual southern right whales females and calves. Individuals with R^2 values below 0.5 (red vertical dashed lines) were removed from analyses. n=78 individuals.

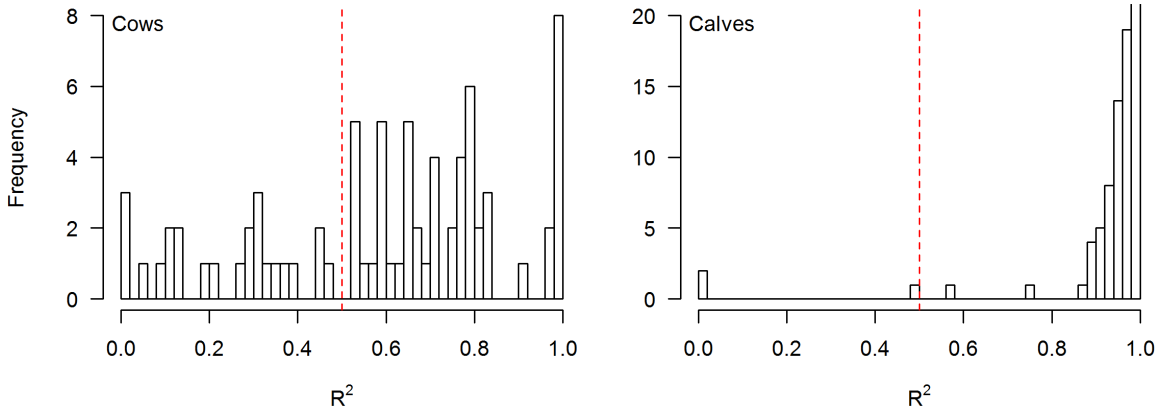

Fig. S6. Calf rate of change in body volume as a function of rate of change in body length ($F_{1,38}$=13.6, P<0.001, R^2=0.26). The dashed lines represent 95% confidence intervals. Calf body condition (CBC) was calculated from the residuals of the linear model. n=40 individuals.

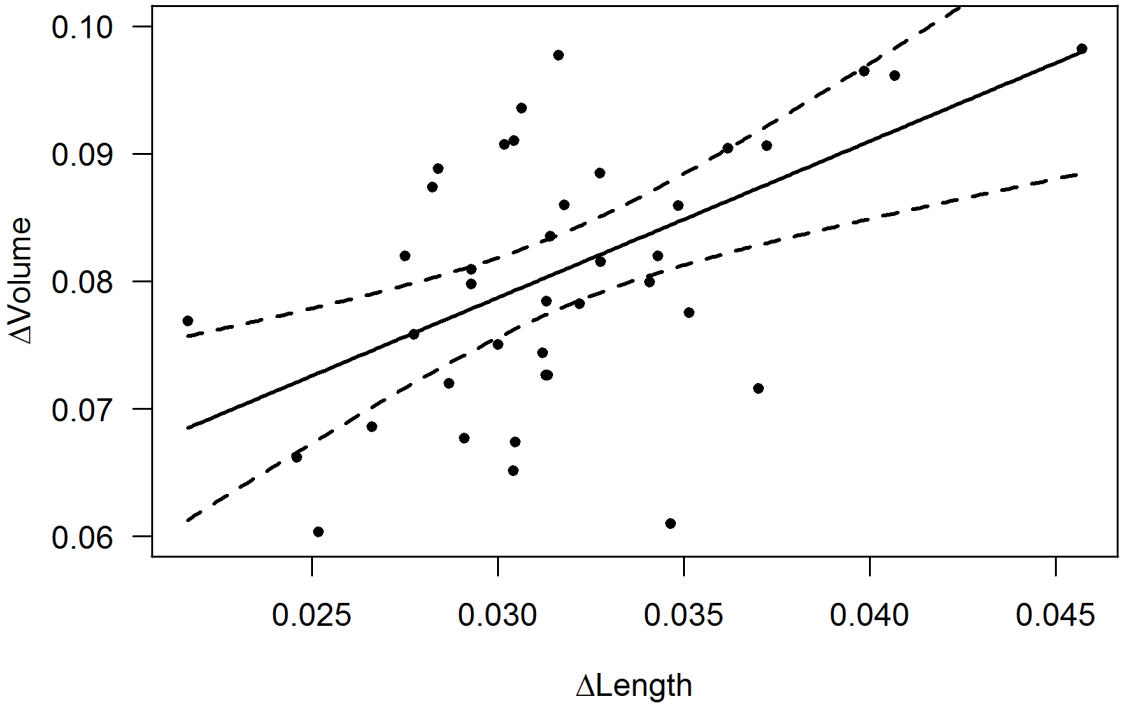

Fig. S7. Calf body volume as a function of body length ($F_{2,590}$=3587, P<0.001, R^2=0.92). The dashed lines represent 95% confidence intervals. The dotted horizontal red line represents the body volume at birth (1.6m^3) specified in the analyses. n=593 measurements from 40 individuals.

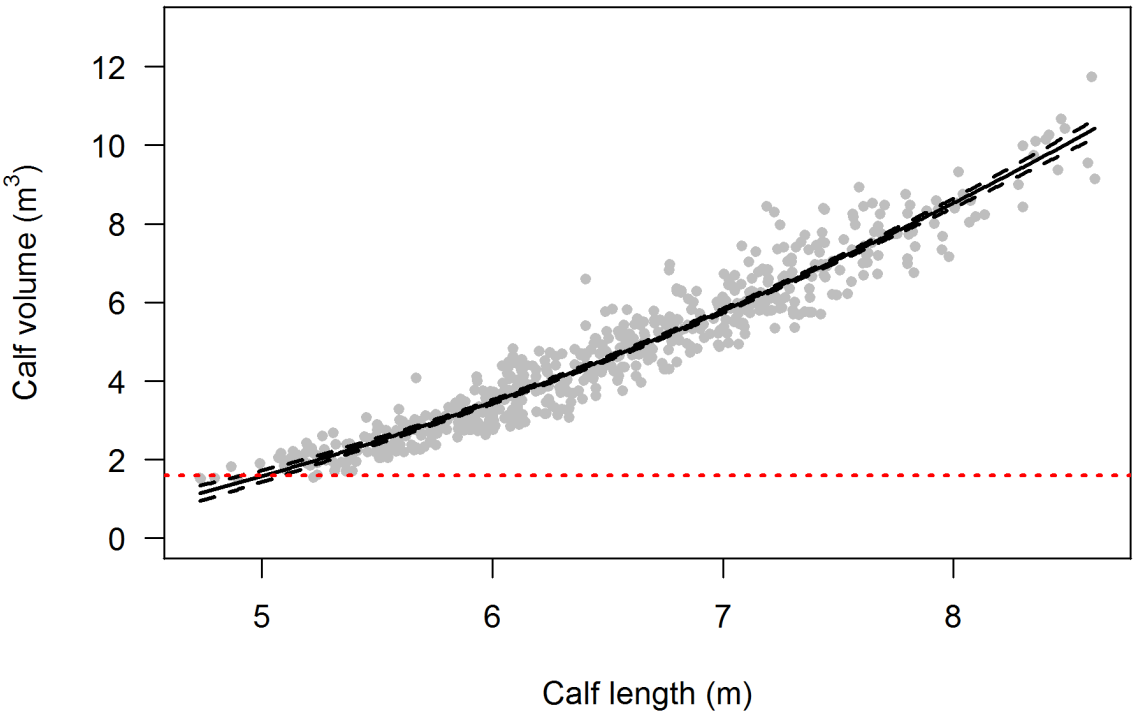

Fig. S8. Maternal body volume at the time of calf birth as a function of maternal body length ($F_{1,38}$=64.1, P<0.001, R^2=0.63). The dashed lines represent 95% confidence intervals. Female body condition (FBC) was calculated from the residuals of the linear model divided by the predicted (expected) values (see main text for details). n=40 individuals.

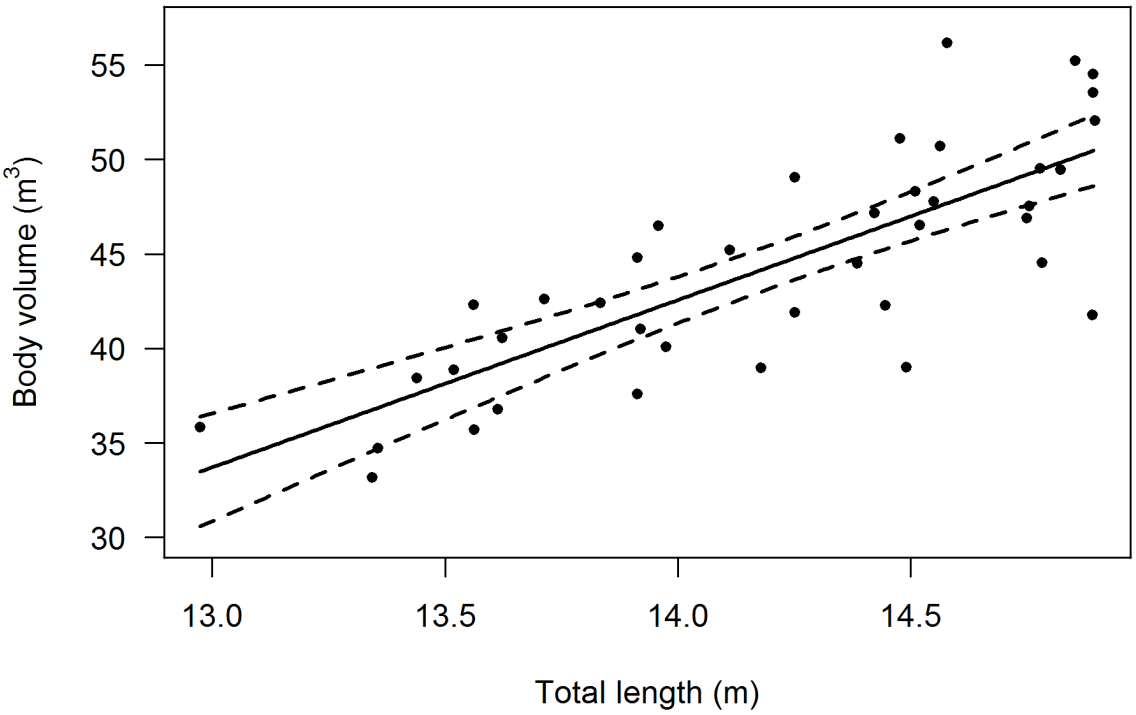

Fig. S9. Unmanned aerial vehicle (UAV) camera measurement errors in (A) Y (i.e. length) and (B) X (i.e. width) as a function of altitude. Three UAVs were used in the experiment (see legend). n=50 measurements.

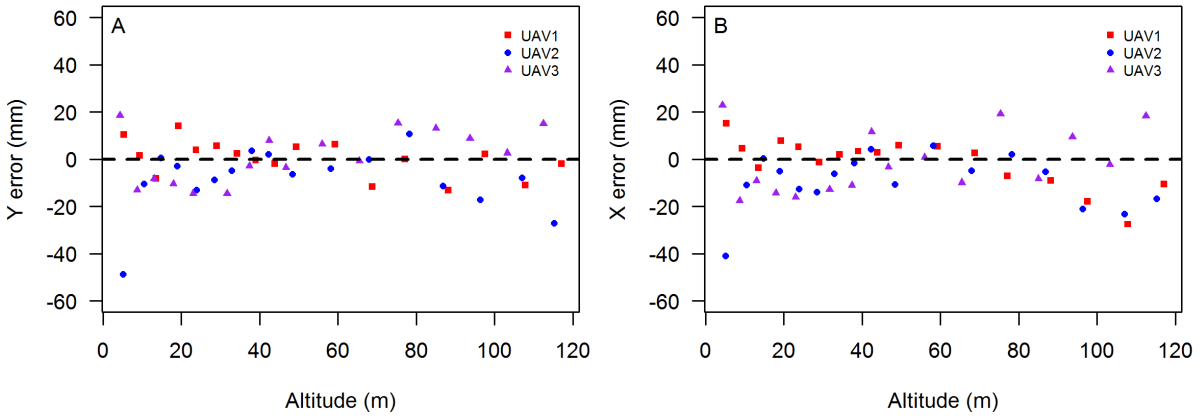

Fig. S10. Coefficient of variation (COV) in (A) body length and (B) body width (at 60% body length from the rostrum) for different body length and width measurability scores, respectively. COV was calculated for each photograph from three independent measurements. Photographs that obtained a body length and/or width measurability score of three were removed from analysis. n=187 photographs.

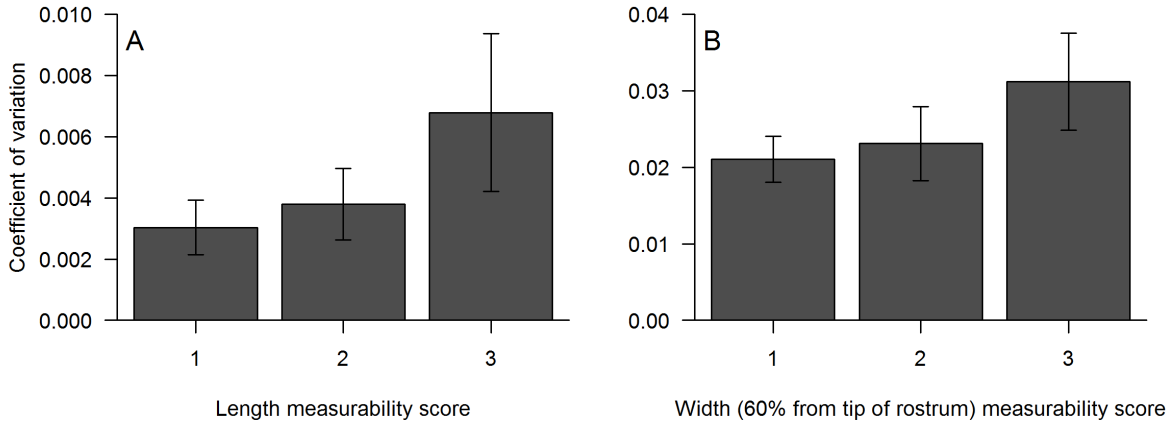

Fig. S11. Measurement error in body width (at 60% body length from the rostrum) from repeated measurements of the same (A) lactating females (n=102 from 34 whales) and (B) calves (n=108 from 36 whales) during the same day. Three measurements were taken of each whale. The solid black line represent the zero line (no error) and the red dashed lines represent the mean measurement error (errors can be both positive and negative).

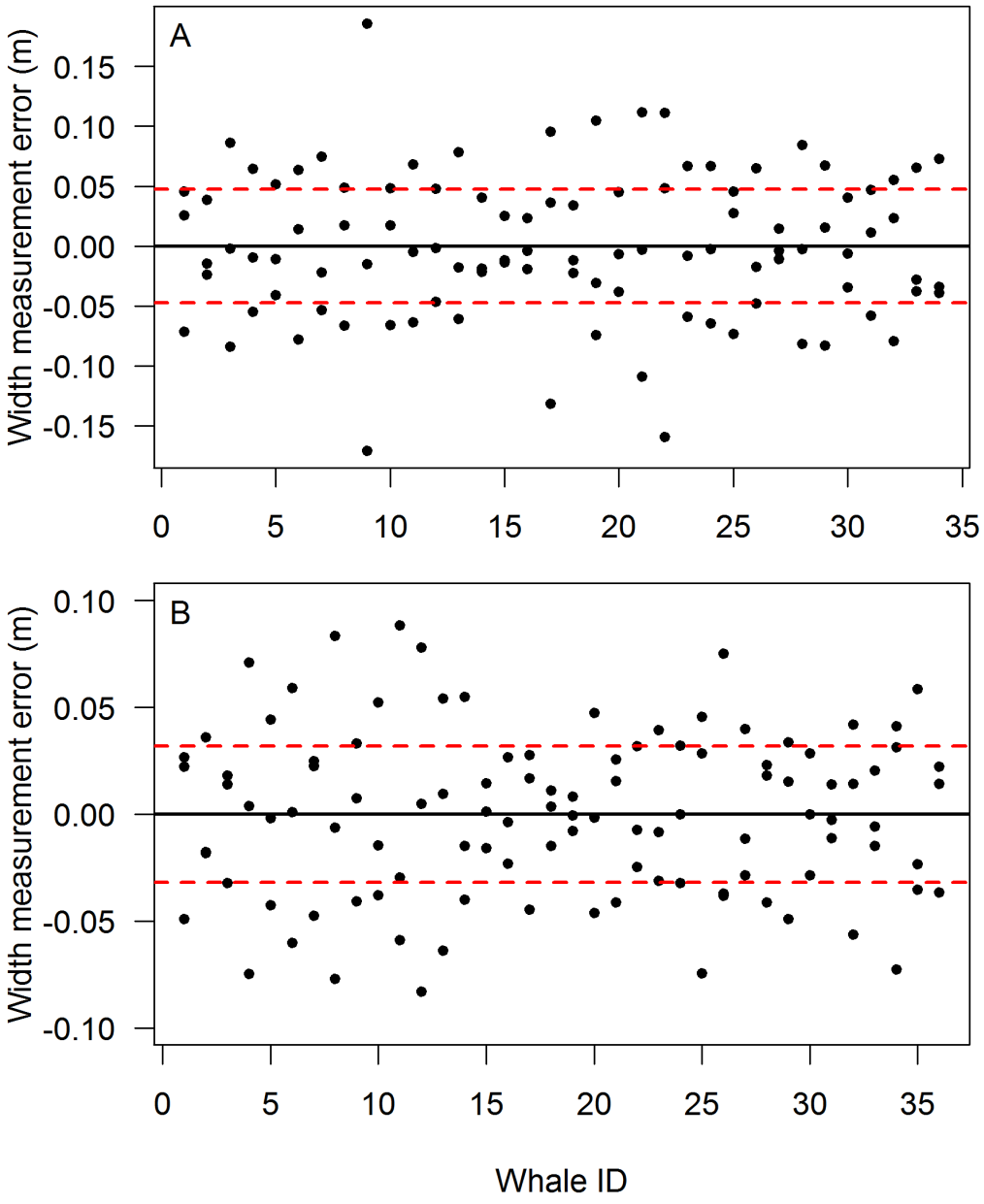

Fig. S12. Sensitivity analysis of measurement errors (range finder errors, within picture measurement errors and between picture measurement errors) showing the density distribution of the model parameter values (slope parameters β) for: (A) the growth rate in calf body volume, (B) the rate of change in maternal body volume, (C) the relationship between rate of change in calf body volume and rate of change in maternal body volume, (D) the relationship between CBC and rate of change in maternal body volume, and the relationship between maternal rate of change in body volume and (E) maternal body length and (F) female body condition, based on 1,000 bootstrapping iterations.

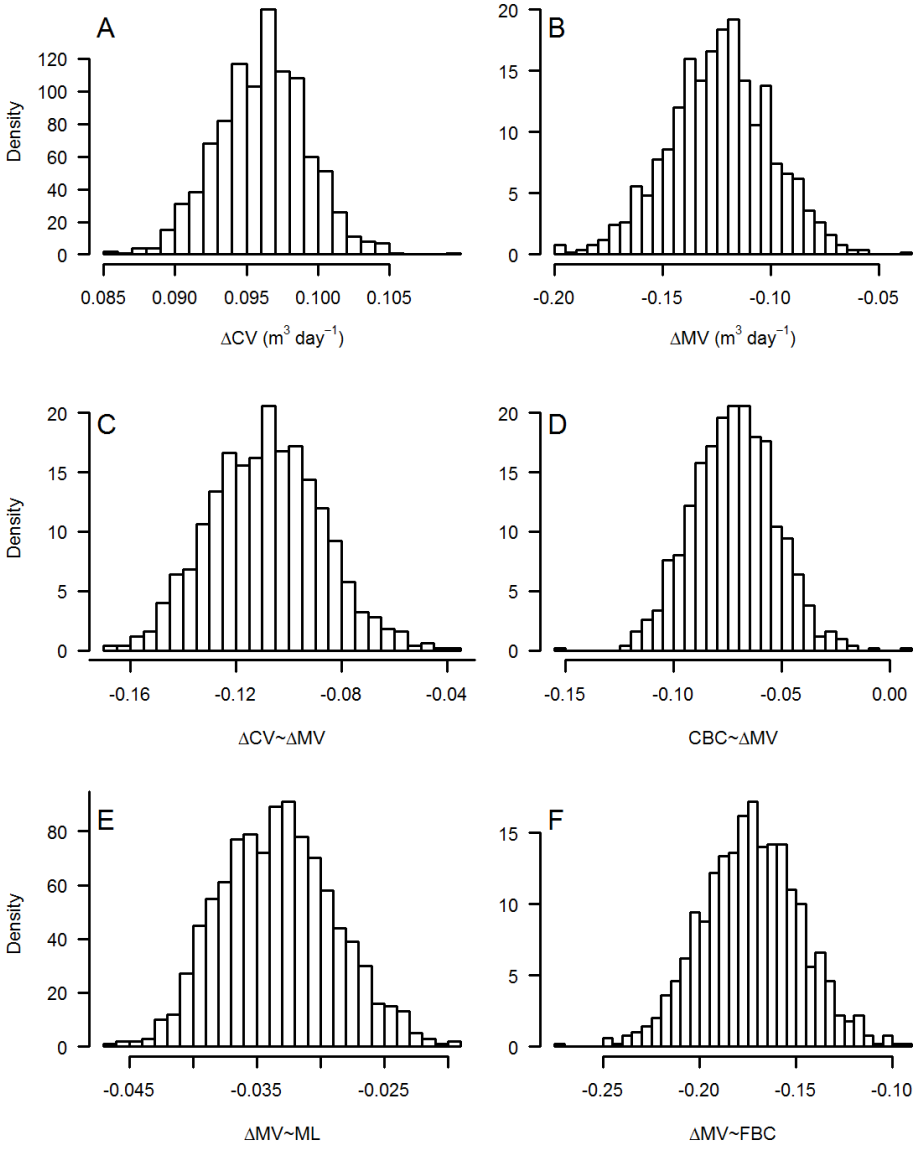

Fig. S13. Number of individual whales measured per day throughout the study period (June 24 - Sept 25). The relative contribution of each reproductive class is given by the colour (see legend). Only cows (black bars) and calves (grey bars) were used in the analyses.

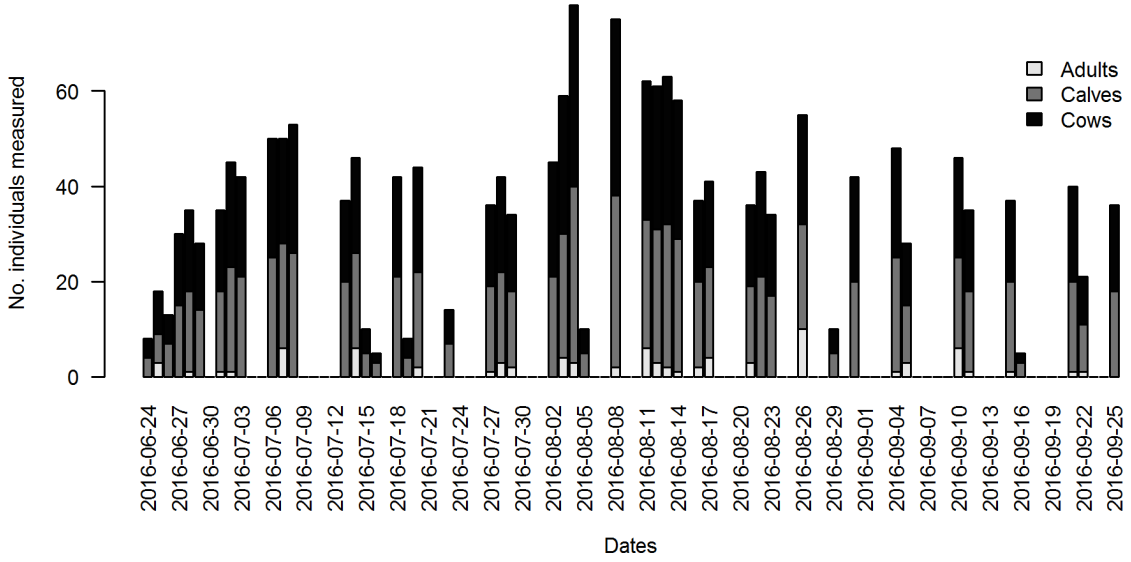

Fig. S14. Frequency histogram showing the number of times (first row) individual southern right whale cows (left column) and calves (right column) were measured and the duration of time (second row) between the first and last measurement.

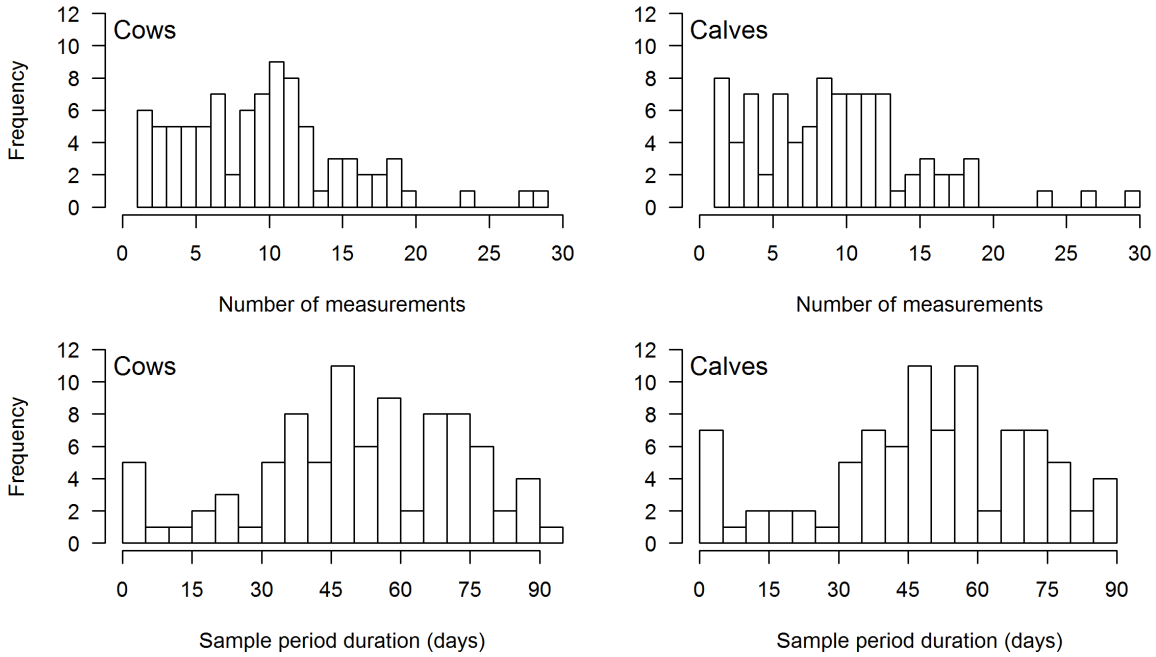

Fig. S15. Calf relative body width (proportion of body length, BL) at 25% BL from rostrum, as a function of days since birth ($F_{3.62,4.53}$=56.84, P<0.001, R^2=0.31). The dashed lines represent 95% confidence intervals. n=593 measurements from 40 individuals.

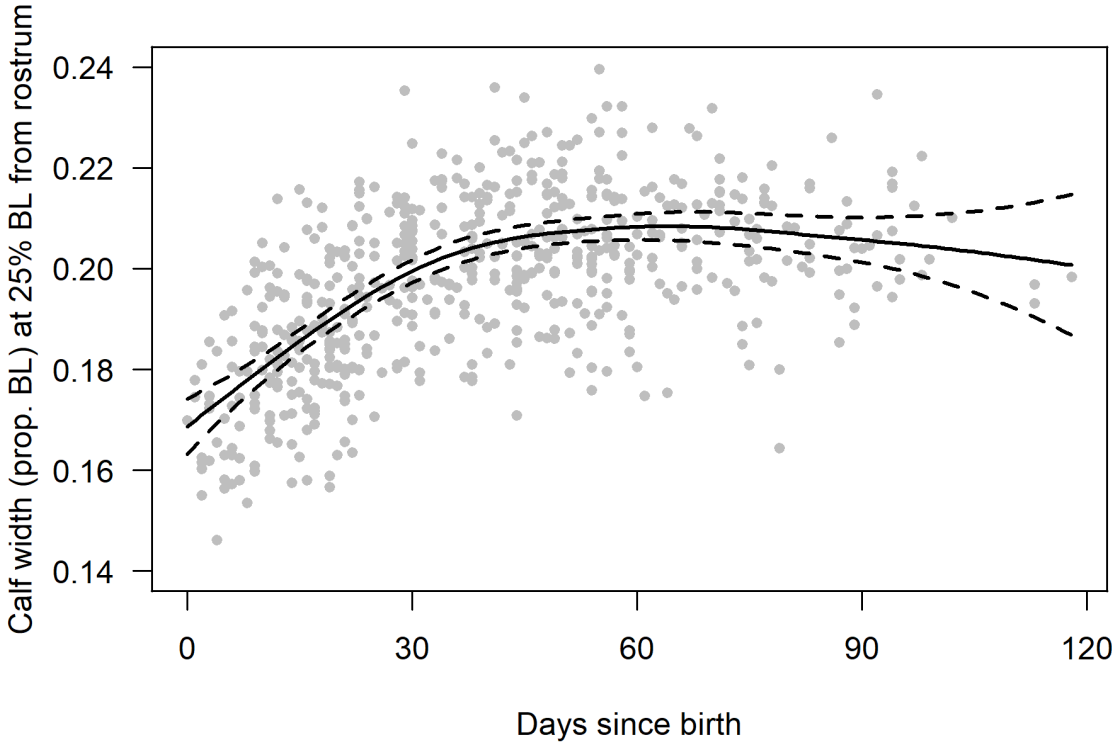

Fig. S16. (A) Calf body volume ($F_{1,591}$=5925, P<0.001, R^2=0.91), (B) body length ($F_{3,589}$=1966, P<0.001, R^2=0.91) and (C) relative body length in proportion to maternal length ($F_{3,589}$=1409, P<0.001, R^2=0.88), as a function of days since birth. Each solid line represents the fitted line from a linear model. (B) and (C) were fitted using cubic polynomial relationships. The dashed lines represent 95% confidence intervals. n=593 measurements from 40 individuals.

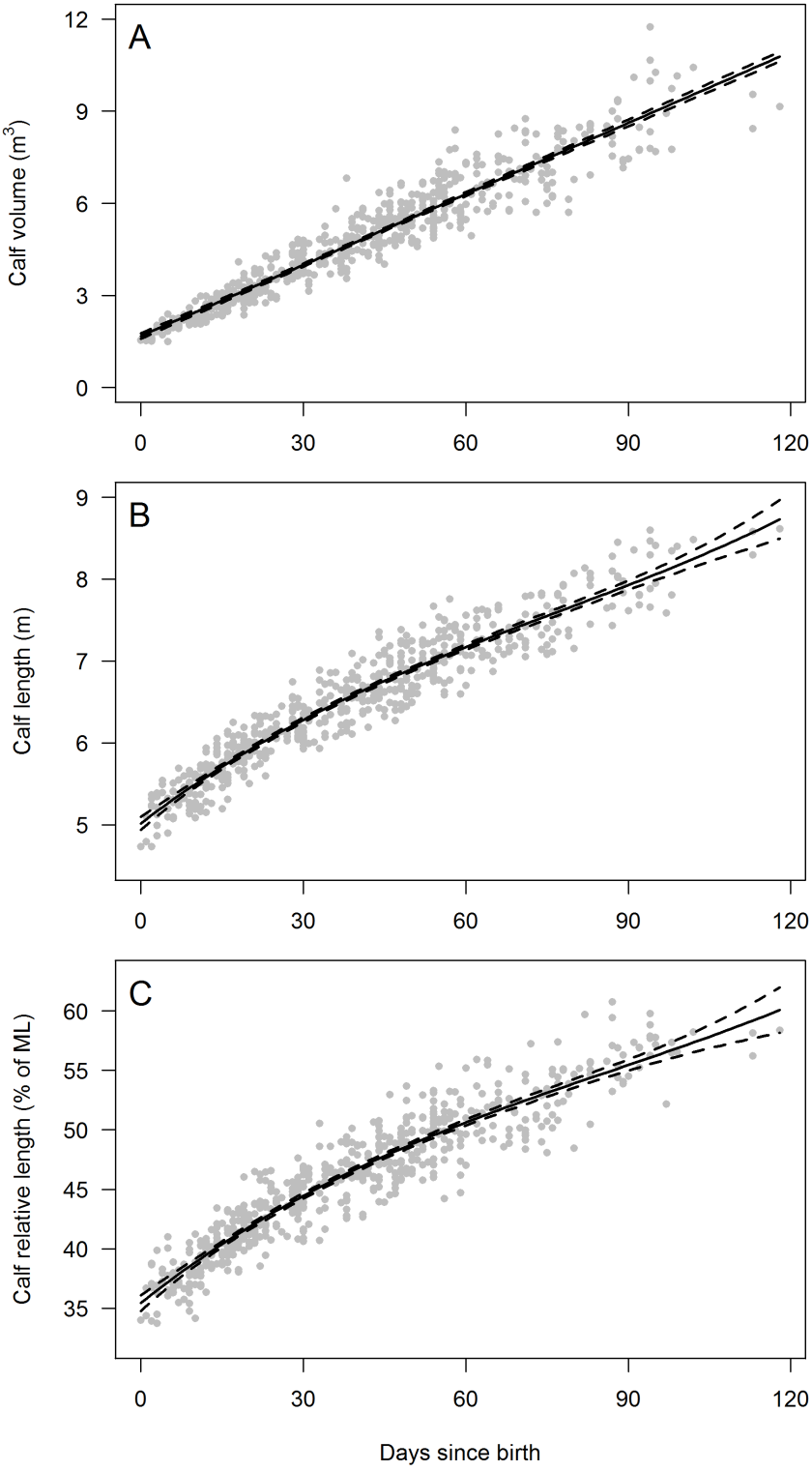

Fig. S17. Frequency distribution of body length of southern right whale lactating females. n=40 lactating females.

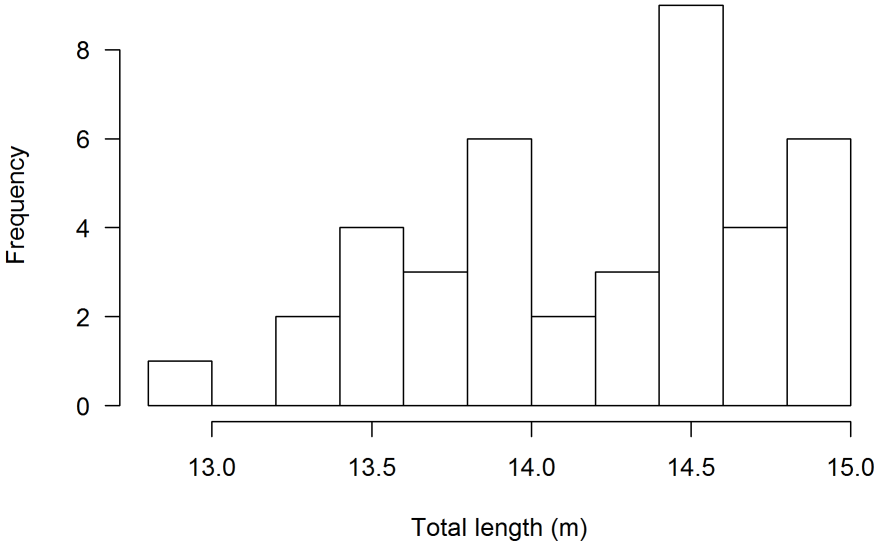

Fig. S18. Frequency distribution of the relative loss in body volume (proportional loss in volume compared to time of birth) of lactating southern right whale females over a 90 day breeding period. n=40 pairs.

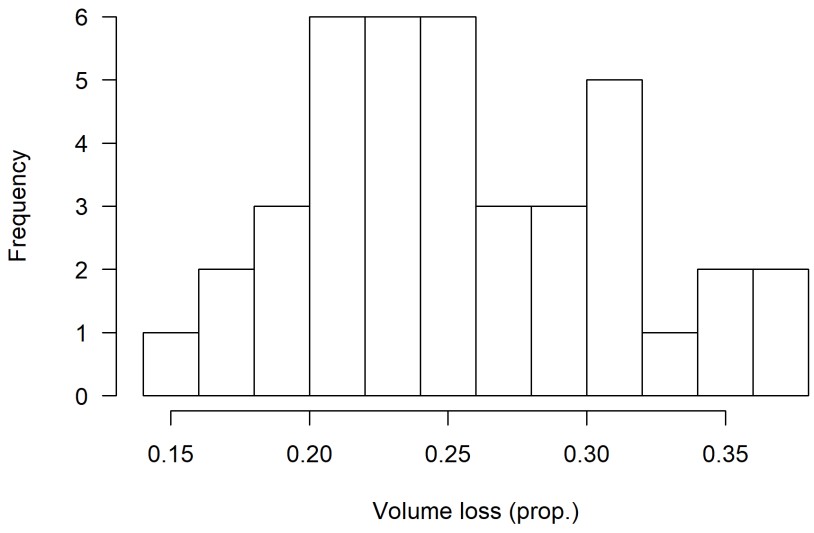

Fig. S19. Frequency distribution of the body volume conversion efficiency (the relative growth in calf volume for every 1 m^3 loss in maternal volume) between southern right whale females and calves. n=40 pairs.

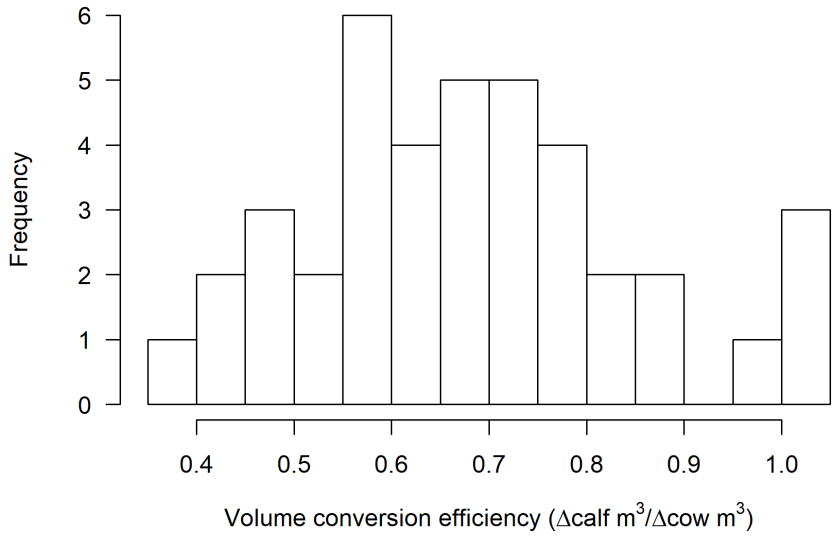

Fig. S20. Maternal rate of loss in body volume as a function of absolute volume at the time of giving birth ($F_{1,38}$=21.3, P<0.001, R^2=0.360). The dashed lines represent 95% confidence intervals. n=40 individuals.

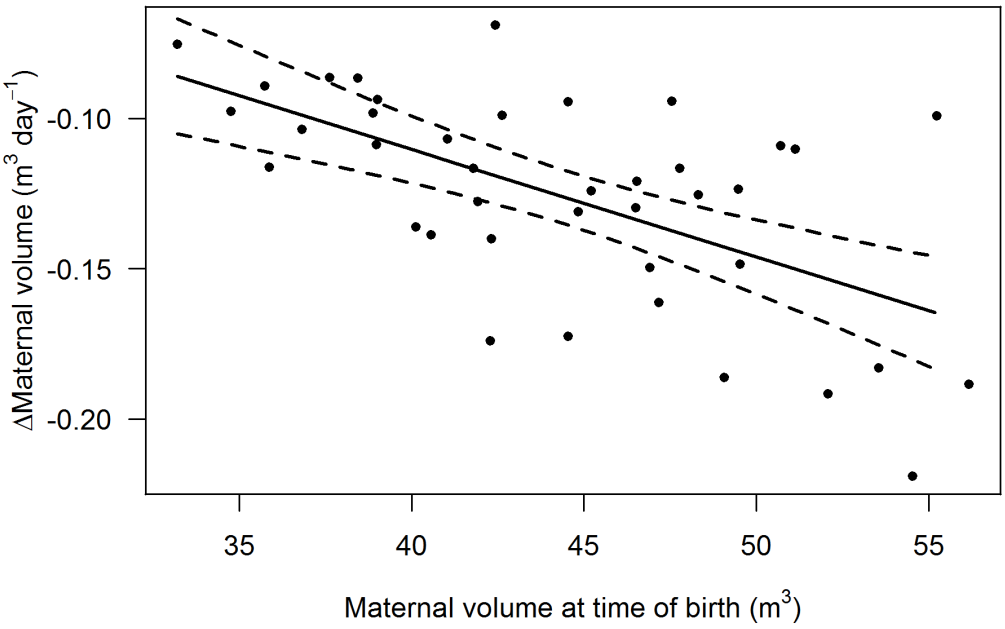

Fig. S21. Intra-seasonal change in body volume of two resting southern right whale females. The black (n=5) and grey (n=6) solid lines represent the fitted values of a linear model fitted to each whale separately.